

UC Davis

UC Davis Previously Published Works

Title

Efficient Low-pH Iron Removal by a Microbial Iron Oxide Mound Ecosystem at Scalp Level Run

Permalink

<https://escholarship.org/uc/item/8b25f9cd>

Journal

Applied and Environmental Microbiology, 83(7)

ISSN

0099-2240

Authors

Grettenberger, Christen L
Pearce, Alexandra R
Bibby, Kyle J
[et al.](#)

Publication Date

2017-04-01


DOI

10.1128/aem.00015-17

Peer reviewed



Efficient Low-pH Iron Removal by a Microbial Iron Oxide Mound Ecosystem at Scalp Level Run

Christen L. Grettenberger,^{a,b} Alexandra R. Pearce,^b  Kyle J. Bibby,^{c,d} Daniel S. Jones,^{b,e} William D. Burgos,^f Jennifer L. Macalady^b

Department of Earth and Planetary Sciences, University of California—Davis, Davis, California, USA^a;
Department of Geosciences, The Pennsylvania State University, University Park, Pennsylvania, USA^b;
Department of Civil and Environmental Engineering, University of Pittsburgh, Pittsburgh, Pennsylvania, USA^c;
Department of Computational and Systems Biology, University of Pittsburgh, Pittsburgh, Pennsylvania, USA^d;
BioTechnology Institute and Department of Earth Sciences, University of Minnesota, Minneapolis, Minnesota, USA^e;
Department of Civil and Environmental Engineering, The Pennsylvania State University, University Park, Pennsylvania, USA^f

ABSTRACT Acid mine drainage (AMD) is a major environmental problem affecting tens of thousands of kilometers of waterways worldwide. Passive bioremediation of AMD relies on microbial communities to oxidize and remove iron from the system; however, iron oxidation rates in AMD environments are highly variable among sites. At Scalp Level Run (Cambria County, PA), first-order iron oxidation rates are 10 times greater than at other coal-associated iron mounds in the Appalachians. We examined the bacterial community at Scalp Level Run to determine whether a unique community is responsible for the rapid iron oxidation rate. Despite strong geochemical gradients, including a >10-fold change in the concentration of ferrous iron from 57.3 mg/liter at the emergence to 2.5 mg/liter at the base of the coal tailings pile, the bacterial community composition was nearly constant with distance from the spring outflow. Scalp Level Run contains many of the same taxa present in other AMD sites, but the community is dominated by two strains of *Ferrovum myxofaciens*, a species that is associated with high rates of Fe(II) oxidation in laboratory studies.

IMPORTANCE Acid mine drainage pollutes more than 19,300 km of rivers and streams and 72,000 ha of lakes worldwide. Remediation is frequently ineffective and costly, upwards of \$100 billion globally and nearly \$5 billion in Pennsylvania alone. Microbial Fe(II) oxidation is more efficient than abiotic Fe(II) oxidation at low pH (P. C. Singer and W. Stumm, *Science* 167:1121–1123, 1970, <https://doi.org/10.1126/science.167.3921.1121>). Therefore, AMD bioremediation could harness microbial Fe(II) oxidation to fuel more-cost-effective treatments. Advances will require a deeper understanding of the ecology of Fe(II)-oxidizing microbial communities and the factors that control their distribution and rates of Fe(II) oxidation. We investigated bacterial communities that inhabit an AMD site with rapid Fe(II) oxidation and found that they were dominated by two operational taxonomic units (OTUs) of *Ferrovum myxofaciens*, a taxon associated with high laboratory rates of iron oxidation. This research represents a step forward in identifying taxa that can be used to enhance cost-effective AMD bioremediation.

KEYWORDS *Ferrovum myxofaciens*, acid mine drainage, environmental microbiology, extremophiles, iron oxidation

Acid mine drainage (AMD) is a devastating and widespread industrial pollution problem (1–6). The effects of AMD are felt especially hard in the Appalachian Plateau in the eastern United States, where over 8,000 km of streams are polluted by

Received 5 January 2017 Accepted 10 January 2017

Accepted manuscript posted online 13 January 2017

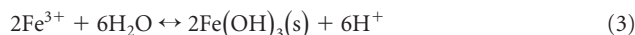
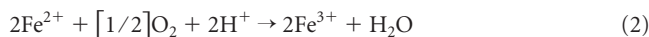
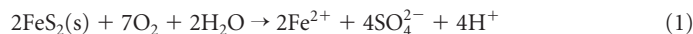
Citation Grettenberger CL, Pearce AR, Bibby KJ, Jones DS, Burgos WD, Macalady JL. 2017. Efficient low-pH iron removal by a microbial iron oxide mound ecosystem at Scalp Level Run. *Appl Environ Microbiol* 83:e00015-17. <https://doi.org/10.1128/AEM.00015-17>.

Editor Robert M. Kelly, North Carolina State University

Copyright © 2017 American Society for Microbiology. All Rights Reserved.

Address correspondence to Jennifer L. Macalady, jlm80@psu.edu.

AMD. Many of these streams are located in Pennsylvania, where a long history of coal mining has set the stage for a major AMD problem (7). Acid mine drainage occurs when pyrite or other sulfide minerals exposed by mining are exposed to water and oxygen and react to produce ferrous iron and sulfuric acid via the following reactions [where "(s)" means "solid"]:



Equation 1 describes a frequent event in which oxygen is consumed in groundwater and Fe(II) is mobilized, resulting in AMD springs that emerge anoxic and mildly acidic (for examples, see references 8 to 11). Iron oxidation and iron oxide precipitation (equations 2 and 3) occur immediately downstream from the springs, spatially distant from pyrite-containing coal deposits. Due to the legacy of coal mining in the Appalachians, AMD spring discharges are extremely common (2).

Acid mine drainage springs and associated iron oxide mounds are chemically and physically heterogeneous. They differ in iron oxidation rates (for examples, see references 8, 9, 12, and 13), geochemistry, and microbial community composition. Previous work suggests that the AMD bacterial community composition is strongly influenced by pH and the concentration of ferrous iron (10, 14). Differences in bacterial community composition can account for some of the observed variation in iron oxidation rates (11, 15). However, it is clear that we require more detailed knowledge of the physical and geochemical variables that control bacterial population distributions (ecological niches), especially at sites where Fe(II) oxidation rates are high.

Iron oxidation rates at Scalp Level Run (Cambria County, PA) (Fig. 1) are 10 times greater than those at other sites in Pennsylvania and the Iberian Pyrite Belt (13). We hypothesized that a unique bacterial community is responsible for the rapid oxidation of Fe(II) at Scalp Level Run. We used fluorescence *in situ* hybridization (FISH) and high-throughput 16S rRNA gene sequencing to identify and quantify bacterial populations at Scalp Level Run and field geochemical methods to investigate *in situ* the environmental parameters that control their distribution.

RESULTS

Geochemistry. The average concentration of ferrous iron in Scalp Level Run decreased from 57.3 mg/liter at the emergence to 2.5 mg/liter at the base of the coal tailings pile (SL 82; Fig. 2A; see also Table S1 in the supplemental material). Similarly, the concentration of total iron decreased from 70 mg/liter at the emergence to 49.7 mg/liter at SL 8.5. Total iron then increased to 63.5 mg/liter at SL 25 before continuing to decrease to 10.6 mg/liter at the base of the coal tailings pile (Fig. 2A; Table S1). The pH varied from 2.77 at SL 82 to 2.96 at SL 8.5 (Fig. 2A; Table S1). Dissolved oxygen increased rapidly from 0.5 mg/liter at the emergence to 9.1 mg/liter at SL 25 and then decreased to 8.4 mg/liter at SL 47 and SL 82 (Fig. 2B; Table S1). Temperature and oxidation-reduction potential (ORP) increased from the emergence, 13.3°C and 386.2 mV, respectively, to the base of the coal tailings pile (20.7°C and 491.7 mV) (Fig. 2B; Table S1).

Community composition. MiSeq Illumina bacterial sequence tags were obtained for SL 8.5, SL 25, and SL 82 samples (Fig. 3A). Between 67% and 92% of the sequences at each site fell within the *Proteobacteria*. Within the *Proteobacteria*, the *Betaproteobacteria* order *Ferroviales* was the most common (49 to 63% of sequences). There were two abundant operational taxonomic units (OTUs) within the *Ferroviales*. Both were closely related to strains of the autotrophic Fe(II) oxidizer *Ferrovum myxofaciens*. The most abundant *Ferrovum* OTU was closely affiliated with isolate EHS8 (KC155322.1; 100% similarity), and the second OTU was most closely related to *Ferrovum* sp. PN-J185 (KC677657.1; 97% similarity). The *Gammaproteobacteria* order *Xanthomonadales* was also abundant and composed 9 to 24% of the sequences (Fig. 3A). All *Xanthomonadales*

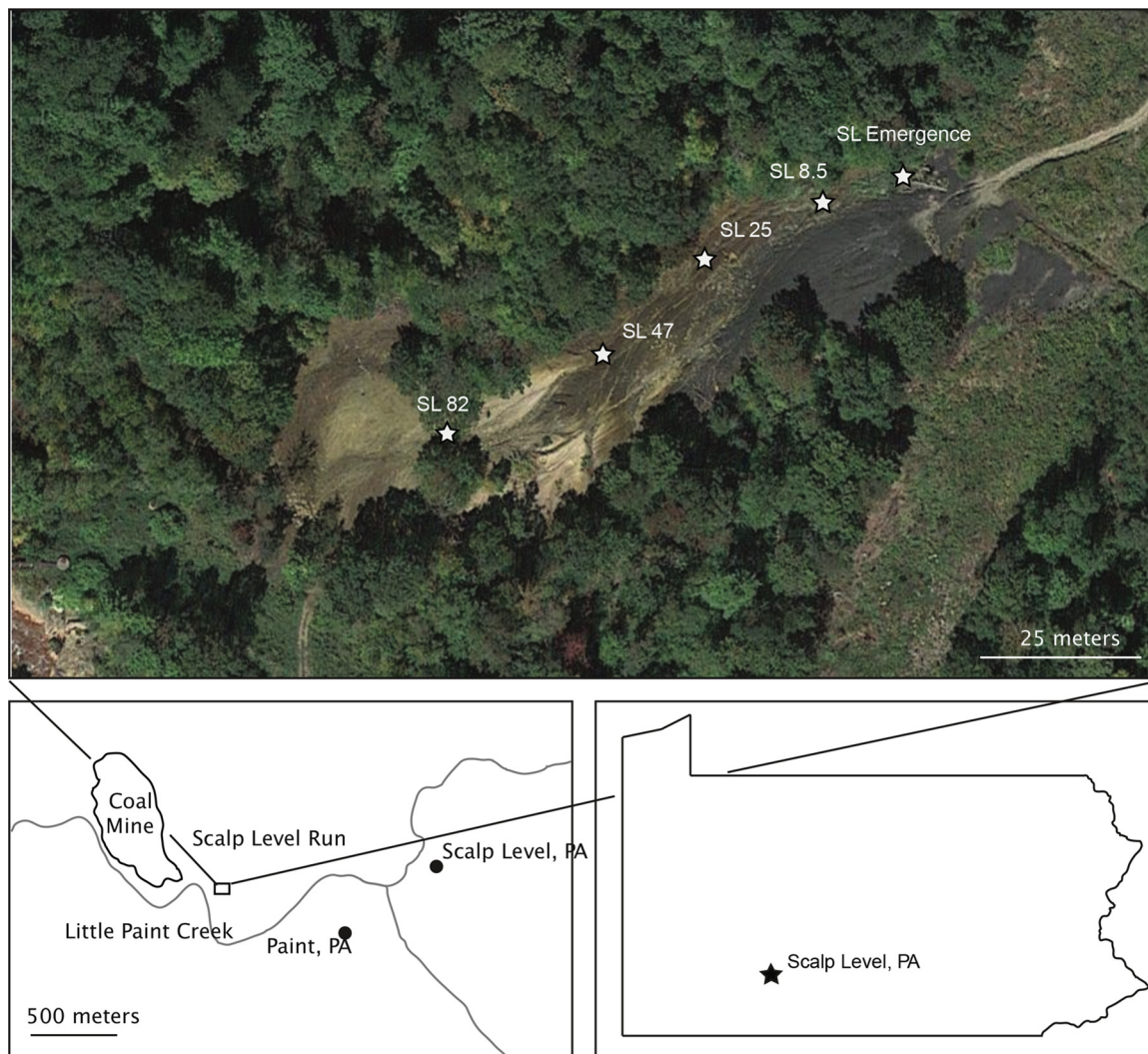


FIG 1 Aerial view of site and sampling locations. (Top base map from Google Maps.) Sampling locations are indicated with stars. AMD effluent flows from the emergence at the top right corner of the figure down the mound until it joins Little Paint Creek on the bottom left.

OTUs were classified as *Xanthomonadales*. The most abundant *Xanthomonadales* OTU was most closely related to *Metallibacterium scheffleri* strain DKE6, an anaerobic Fe(III) reducer (16) (NR_118103.1; 100% similarity). The *Alphaproteobacteria Rhodospiralles* were also common (1 to 18% of sequences). The most abundant *Rhodospiralles* OTU was closely related to the heterotrophic acidophile *Acidiphilium rubrum*.

The phylum *Acidobacteria* was the second most abundant phylum after *Proteobacteria* and was more abundant in SL 25 (7% of bacterial sequences) than in SL 8.5 and 82 (3 and 1% of bacterial sequences, respectively). *Chloroflexi* and *Planctomycetes* were present in all libraries. Rare sequences related to *Cyanobacteria* were present at all sites (<1%). The most abundant cyanobacterial OTU was affiliated with the *Melainabacteria*, a basal group of nonphotosynthetic *Cyanobacteria* (17). Chloroplast sequences were found at all sites and increased in abundance downstream from SL 8.5 (23% of total sequences) to SL 85 (39% of total sequences; see Fig. S1 in the supplemental material). Chloroplast sequences were identified as *Stramenophiles*, *Streptophyta*, *Euglenozoa*, or *Chlorophyta*. *Stramenophiles* were the most abundant. The abundance of chloroplasts from *Euglenozoa* decreased from SL emergence to SL 82. Chloroplast sequences from *Chlorophyta* were present only in SL 25 and SL 82. Chloroplast sequences were removed from the data set for bacterial community composition analyses presented above.

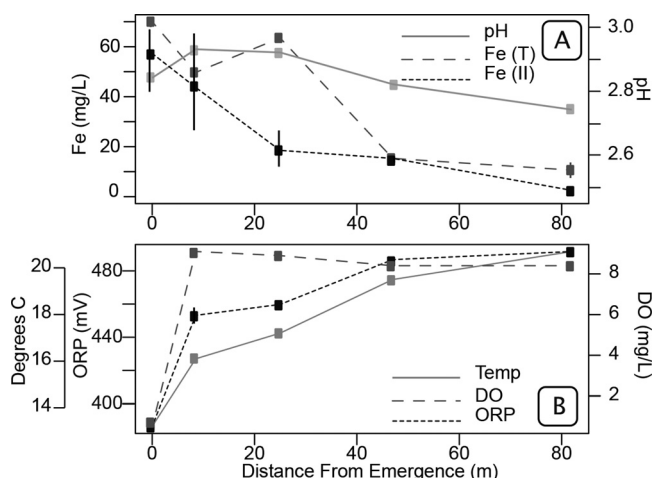


FIG 2 Geochemical profiles at Scalp Level Run. (A) pH (solid gray line) and concentrations of total iron (gray dashed line) and ferrous iron (black dashed line). (B) Temperature (gray solid line), dissolved oxygen (gray dashed line), and ORP (black dashed line).

Fluorescence *in situ* hybridization was used to quantify the relative abundance of common AMD bacterial groups, including *Ferroplasma* spp. (Ferri643 probe), acidophilic *Gallionella* (Gal177 probe), *Acidithiobacillus ferrooxidans*, and an AMD clade of *Xanthomonadales* (Fig. 4; Table 1). The *Betaproteobacteria* were the most abundant group detected by FISH and accounted for 41 to 53% of total bacterial cells. The *Betaproteobacteria* taxon *Gallionella* was not detected at any sample location. The *Ferritrophicum* probe targets a portion of the ribosome that Fuchs et al. (18) classify as a class V region, indicating that a probe in that region is only 6% to 20% as bright as a reference probe. In fact, the probe was too dim to accurately count cells using standard FISH protocols,

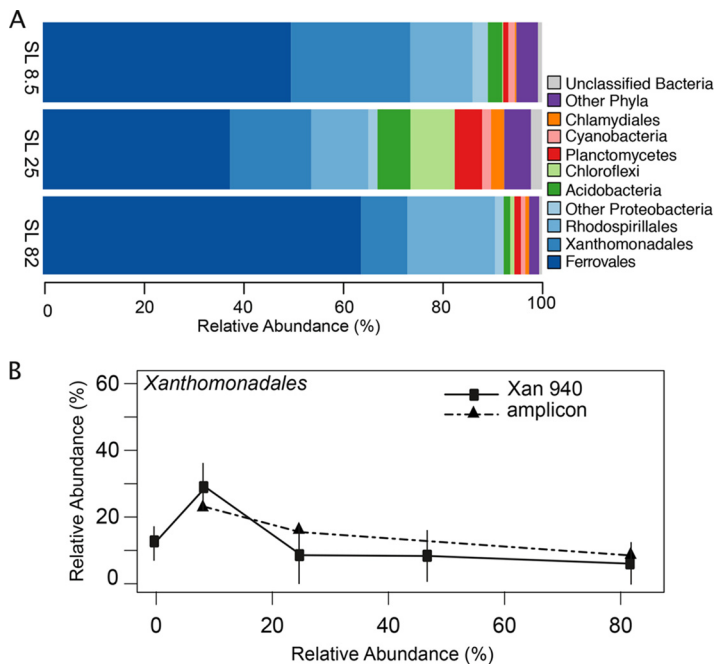


FIG 3 Community composition at Scalp Level Run determined by Illumina sequence tags and FISH. Cell counts are expressed as percentages of Eubmix-stained cells. (A) Bacterial community composition using Illumina sequence tags (relative abundance as a percentage of total bacterial sequences). The *Proteobacteria* (blue) are subdivided into orders, and the rest are shown as phyla. (B) *Xanthomonadales* and Xan940 probe results for Illumina sequence tags (dot-dashed line) and FISH (solid line).

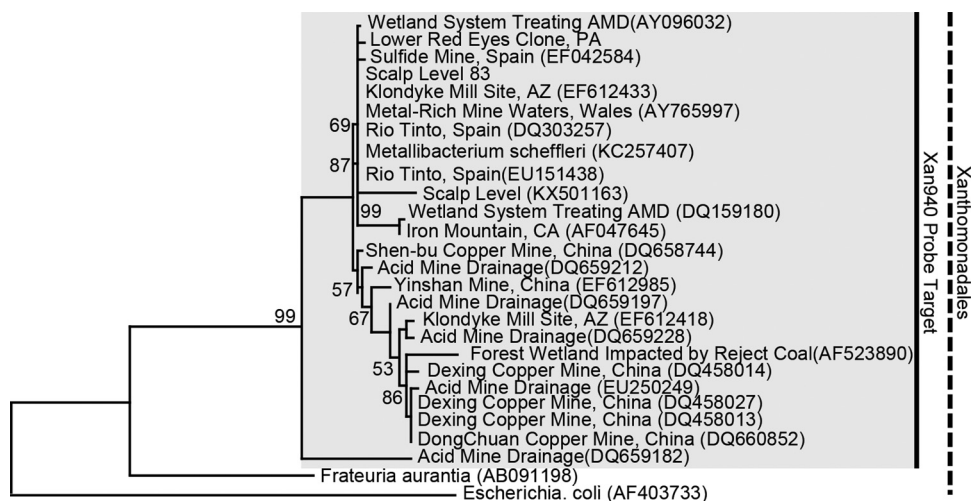


FIG 4 *Xanthomonadales* phylogenetic tree with sequences from Pennsylvania and other AMD sites. The targets of the FISH probe Xan940 are in the gray box. The order *Xanthomonadales* is indicated by a dashed line. The percentages of replicate trees in which the associated taxa clustered together in the bootstrap test (1,000 replicates) are shown next to the branches. Bootstrap values below 50% are omitted.

and we therefore excluded *Ferrirophicum* from FISH-based analyses. *Ferrovum* spp. composed between 3% and 35% of Eubmix-stained cells. This taxon steadily decreased from the emergence to the base of the pile, except at SL 8.5, where the relative abundance sharply decreased (Fig. 5A). Unidentified betaproteobacterial sequences increased from 5% of Eubmix-stained cells at the emergence to 49% at the base of the tailings pile. The *Xanthomonadales* were the second most abundant population detected by FISH and made up between 6% and 29% of the community. The relative abundance of the *Xanthomonadales* was between 6% and 13% across the site, except at SL 8.5, where it composed 29% of the community (Fig. 3B). The *Gammaproteobacteria* genus *Acidithiobacillus* was not detected by FISH at any sampling site.

DISCUSSION

The bacterial community at Scalp Level Run was primarily composed of taxa common to other AMD sites in Pennsylvania and across the globe, including those in the orders *Rhodospirales* (*Alphaproteobacteria*), *Xanthomonadales* (*Gammaproteobacteria*), and *Ferrovales* (*Betaproteobacteria*) (for examples, see references 10, 11, 19, 20, and 21). The *Xanthomonadales* at Scalp Level Run were closely related to other sequences from AMD sites, including in the Rio Tinto, Spain (22), in South Korea (23), and in the United States (9, 10). Acid mine drainage-associated *Xanthomonadales* sequences made

TABLE 1 FISH probes used in this study

Probe name	Sequence (5'-3')	Formamide (%)	Specificity	Label ^a	Source or reference
Dapi		0-50	All DNA		
EUB338	GCT GCC TCC CGT AGG AGT	0-50	Most <i>Bacteria</i>	FITC	52
EUB338-II	GCA GCC ACC CGT AGG TGT	0-50	<i>Planctomycetales</i>	FITC	53
EUB338-III	GCT GCC ACC CGT AGG TGT	0-50	<i>Verrucomicrobiales</i>	FITC	53
THIO1	GCG CTT TCT GGG GTC TGC	35	<i>Acidithiobacillus</i> spp.	Cy-3	54
Ferri643	ACA GAC TCT AGC TTG CCA	35	<i>Ferrovum</i> spp.	Cy-3	14
Gal 177	TCC CCC TCA GGG CAT A	20	<i>Gallionella</i> spp. (from AMD)	Cy-3	13
cGal 177	TCC CCC TCA GGG CTT A	20	Competitor for Gal177	Cy-3	13
Xan 940	GCG CGT TTC GCT CCC GAT	30	<i>Xanthomonadales</i> spp. from AMD	Cy-3	This study
Ferri836	TAC CAA AGA GGT CAC CCT C	30	<i>Ferrirophicum</i> spp. from AMD	Cy-3	This study
Bet42a	GCC TTC CCA CTT CGT TT	35	Most <i>Betaproteobacteria</i> and some <i>Gammaproteobacteria</i>	Cy-3	55
cBet42a	GCC TTC CCA CAT CGT TT	35	Most <i>Gammaproteobacteria</i> ; used as competitor for Bet42a	None	55

^aFITC, fluorescein isothiocyanate.

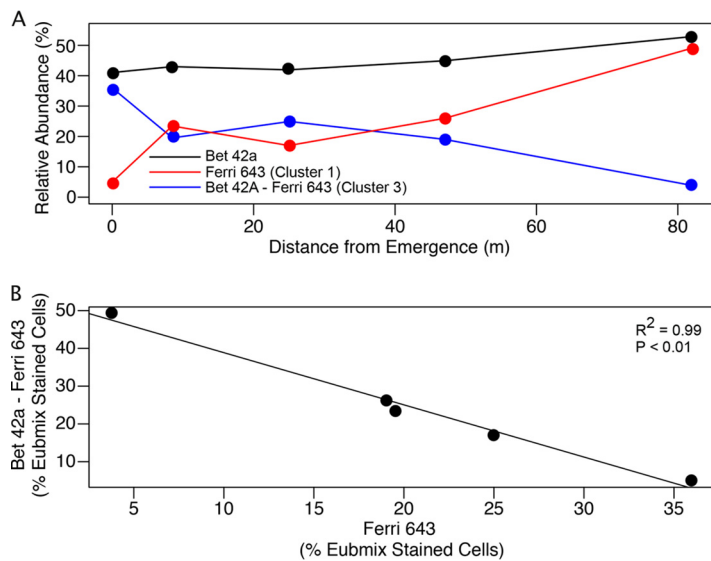


FIG 5 (A) *Ferroviales* and Bet42a probe. The two abundant *Ferrovum* species OTUs are indicated by red (*Ferrovum* cluster 1) and blue (*Ferrovum* cluster 3) lines. (B) Relationship between *Ferrovum* cluster 1 and *Ferrovum* cluster 3 (unknown *Betaproteobacteria*) taxa.

up a monophyletic clade nested within *Xanthomonadales* (Fig. 4). The AMD clade was most closely related to cultivated strain WJ2, a moderately acidophilic Fe(II) oxidizer isolated from an AMD wetland remediation site near Cornwall, England (24). This taxon was also abundant (23% to >50%) in the surface and subsurface of the Mushroom Farm AMD mound in Ohio, USA (25). Nearly all the sequences identified as *Rhodospirillales* fell within the genus *Acidiphilium*, a heterotrophic iron-reducing *Alphaproteobacterium*. This taxon is commonly found in AMD sites, including the Dabaoshan Mine, China (26), and the Rio Tinto watershed (27).

The most abundant order at Scalp Level Run was the *Ferroviales*. There were two abundant OTUs from this order, and these OTUs fell within different clusters of the *Ferroviales* as defined by Tischler and others (28). The first OTU was contained within cluster 1 of the *Ferroviales*, and the second OTU fell within cluster 3 (Fig. 6). The cluster 1 sequence had no mismatches to the Ferri643 probe, whereas the cluster 3 sequence had a one-base-pair mismatch to the probe and therefore would not have been visualized in our FISH experiments. Two distinct *Ferroviales* sequences were found in the clone libraries, but neither of these sequences is affiliated with cluster 3 and both have no mismatches to the Ferri643 probe (Fig. 6).

We identified two abundant species of *Betaproteobacteria* in the amplicon data sets.

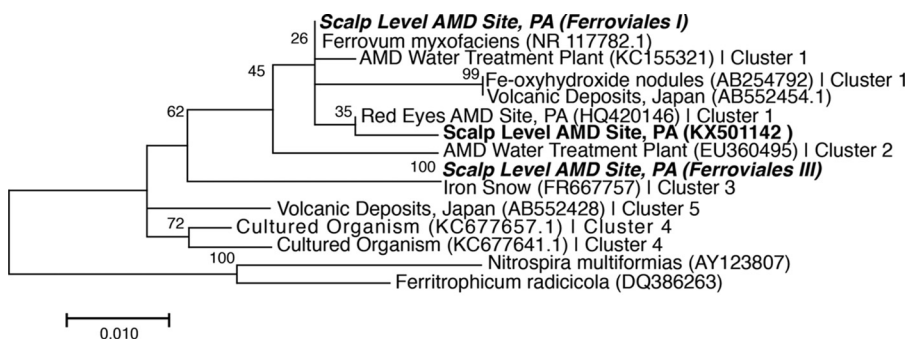


FIG 6 Molecular phylogenetic analysis of *Ferroviales* sequences by maximum likelihood. Nearly full-length sequences from clone libraries are shown in bold. Representative sequences from sequence tags are shown in bold italics. Sequences from the analysis of Tischler et al. (28) are labeled with the corresponding clusters. Bootstrap values (1,000 replicates) are shown next to the branches.

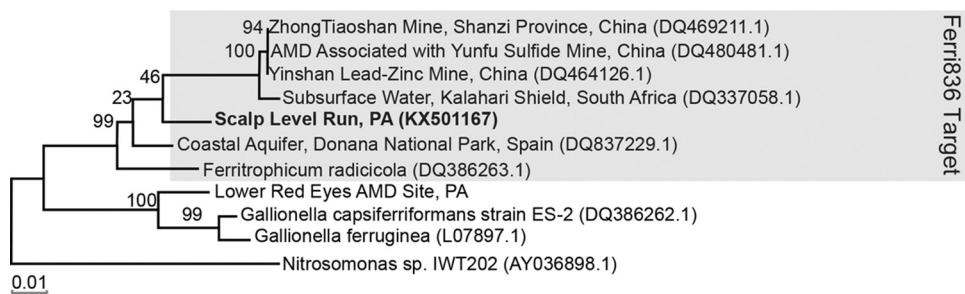


FIG 7 *Ferritrophicum* phylogenetic tree. The sequence from Scalp Level Run is indicated in bold. The targets of the FISH probe Ferrit836 are in the gray box. Numbers indicate the bootstrap support for each node.

Both were members of the genus *Ferrovum*. We expected that the relative abundance of *Ferrovum* spp. in the amplicon data set would equal the relative abundance of *Ferrovum* identified by FISH. However, they were not equivalent; the relative abundance of *Ferrovum* as calculated using FISH was lower than the abundance in the amplicon data set. The discrepancy between the FISH and amplicon data sets likely results from a one-base-pair mismatch between the *Ferrovum* probe and the corresponding 16S rRNA gene sequence in the cluster 3 *Ferrovum* OTU.

The relative abundance of *Betaproteobacteria* (Bet42a) identified by FISH was approximately equal to the combined abundance of the two *Ferrovum* OTUs retrieved from the amplicon data set (Fig. 5A). This is consistent with the result that no other abundant *Betaproteobacteria* were detected in the sequence tag or clone libraries. Thus, the betaproteobacterial community was composed almost exclusively of *Ferrovum* phylotypes. We therefore used the relative abundance of *Betaproteobacteria* as a proxy for the total abundance of *Ferrovum* spp. in the FISH data set and calculated the relative abundance of the cluster 3 *Ferrovum* isolates by difference (see Table S2 in the supplemental material). Using this approach, we found that the relative abundances of the cluster 1 and cluster 3 *Ferrovum* phylotypes are inversely correlated in FISH analyses ($R^2 = 0.99$; $P < 0.01$), with cluster 1 more abundant near the spring emergence and cluster 3 more abundant at the base of the iron mound. Both temperature and pH vary across the iron mound, and both of these parameters are found to influence the growth rate of *F. myxofaciens* PG3, the type strain of *Ferrovum* (29). These factors may be controlling the distribution of *Ferrovum* in separate niches across the Scalp Level Run iron mound.

The only non-*Ferrovum* betaproteobacterial sequence in our clone library fell within the order *Ferritrophicales*, and this order was not abundant in the sequence tag libraries (<0.1%). The *Ferritrophicales* are *Betaproteobacteria* related to the *Gallionellales*, *Ferrovales*, and *Rhodocycales* (29). The sequence that we retrieved from Scalp Level Run was closely related to the Fe(II) oxidizer *Ferritrophicum raditicola* (Fig. 7) and has not been detected at other Pennsylvania AMD sites. *Ferritrophicum raditicola* is an Fe(II) oxidizer isolated from plant roots near an AMD stream (30). Other sequences closely related to *Ferritrophicum raditicola* have been retrieved from the Yunfu sulfide mine (31) and Yinshan lead-zinc mine, China (32), the Carnoulès acid mine drainage, France (33), and La Zarza, Spain (34). *Ferritrophicum* species are not abundant in AMD sites studied to date, with few exceptions (35).

Like most acid mine drainage sites, Scalp Level Run hosts both Fe(II)-oxidizing and Fe(III)-reducing populations. Previous research has shown that there are strong oxygen gradients in the first few centimeters of AMD sediments (e.g., reference 25); therefore, it is not surprising to find both iron-reducing and Fe(II)-oxidizing populations in AMD surface sediments. In these sediments, factors that favor the activity of Fe(II)-oxidizing bacteria over iron-reducing populations could increase the net iron oxidation rate, including light or nutrient availability that enhances oxygenic photosynthesis or a lack of organic matter inputs from the surrounding ecosystem or from algal photoautotrophy at the iron mound surface.

Scalp Level Run surface sediments were colonized by eukaryotic phototrophs, including *Stramenophiles*, *Streptophyta*, *Euglenozoa*, and *Chlorophyta*. Oxygenic phototrophs, including these taxa, could enhance iron oxidation at AMD sites by increasing the concentration of dissolved oxygen at the sediment-water interface, thereby altering the depth at which iron reduction occurs in the subsurface of the mound. In this scenario, the net Fe(II) oxidation rate would increase due to both an increase in the rate of iron oxidation and a decrease in the rate of iron reduction. This mechanism could explain the higher Fe(II) oxidation rates in alga-dominated than in alga-poor sites (11). The same mechanism could explain why the field iron oxidation rates at Scalp Level Run were 20 times greater than the rates in dark laboratory chemostats inoculated with sediment from Scalp Level Run (36). However, the phototrophs are also producing organic carbon, which could be used in dissimilatory iron reduction. The influence of phototrophy on the system is likely dependent on the turnover over time of both the carbon and oxygen and the activity of the heterotrophs. We do not have sufficient data to quantify the effect of phototrophy on our system.

The results that we obtained from Scalp Level Run place new constraints on emerging ideas about physical and chemical niches of AMD phylotypes. In the ecological niche model for Fe(II)-oxidizing bacteria described by Brown et al. (14) and Senko et al. (10), pH and the concentration of ferrous iron were strongly correlated with the abundance of Fe(II)-oxidizing bacterial populations in Appalachian AMD. Both pH and the concentration of ferrous iron at Scalp Level Run were lower than at the sites used to construct the niche model. Scalp Level Run also provided a unique opportunity to isolate the effects of ferrous iron concentrations on bacterial communities independent of major changes in pH.

Both FISH and 16S rRNA gene sequence tag data show that the bacterial community composition was largely constant across the Scalp Level Run site (Fig. 3A). Of 42 bacterial orders that were detected at Scalp Level Run, 30 were found at all three sampling locations. These 30 orders made up between 98.9% and 99.9% of the community at each sampling location. Moreover, only eight orders were restricted to a single sampling location and all of these "endemic" orders represented rare populations (less than 0.01% of the community). The constant community composition at Scalp Level Run despite large changes in the concentration of ferrous iron suggests that ferrous iron availability is not an important driver of community composition at Scalp Level Run.

Unlike most other AMD sites in the Appalachian region, pH varies by only 0.2 units across the Scalp Level Run iron mound, whereas the concentration of ferrous iron changes over 1 order of magnitude. This situation presented a unique opportunity to test relationships proposed in earlier work at Appalachian coal mine drainages. Whereas Brown et al. (14) and Senko et al. (10) suggested that AMD populations respond to both pH and [Fe(II)], the Scalp Level Run bacterial community composition does not appear to respond to the large changes in ferrous iron concentrations across the site. However, the majority of the sites used to construct the niche model proposed by Brown et al. (14), Senko et al. (10), and others were above pH 3. The pH at Scalp Level Run is low enough to keep most ferric iron in solution. Under these conditions, the precipitation of iron oxides and production of H⁺ (equation 3) is kinetically inhibited. Therefore, iron oxidation does not immediately lead to a decrease in pH as it does at less acidic AMD springs where ferric iron is insoluble.

Overall, our results indicate that pH is the main controller of the composition of bacterial communities in coal-associated AMD and that *Ferrovum*, acidophilic *Gallionella*-like spp., and *Acidithiobacillus* populations inhabit niches defined by pH, where acidophilic *Gallionella*-like spp. dominate above pH 3.5 and *A. ferrooxidans* is most abundant below pH 3 (Fig. 8). Similarly, Kuang and others found that *Ferrovum* spp. and other *Betaproteobacteria* were predominant in bacterial assemblages in moderate AMD systems whereas the *Alpha*- and *Gammaproteobacteria* and *Nitrospira* were found in more-acidic environments (37).

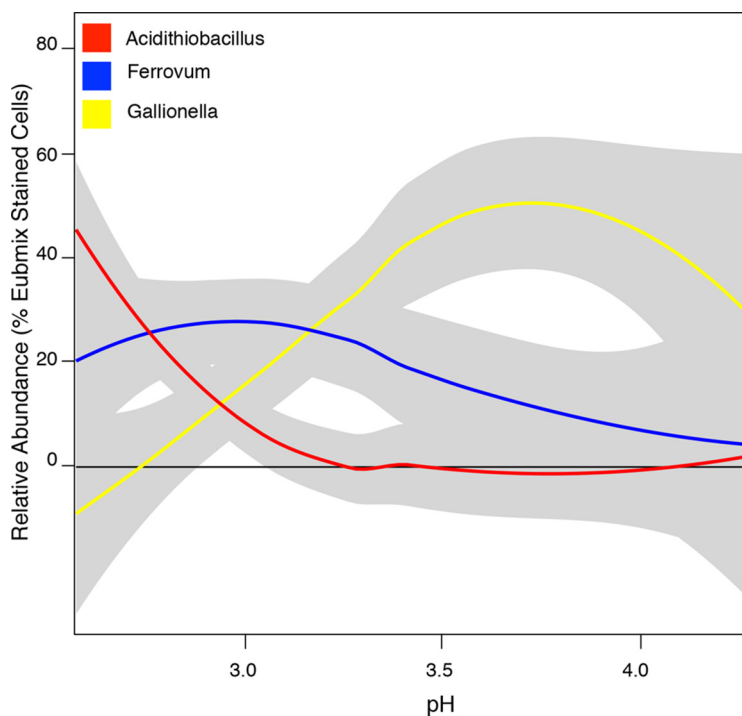


FIG 8 Loess regression line for relative abundance of *Acidithiobacillus* (Thio1), *Ferrovum myxofaciens* (Ferri643), and acidophilic *Gallionella* (Gal177) as determined by FISH. Gray bands show 95% confidence intervals.

Ferrovum myxofaciens appears to be most abundant between pH 3 and 4 but has a broader distribution than either acidophilic *Gallionella*-like spp. or *A. ferrooxidans*. This broad distribution may indicate that *F. myxofaciens* is a more generalist taxon with respect to pH than acidophilic *Gallionella*-like spp. or *Acidithiobacillus* spp. Alternately, an as-yet-undiscovered geochemical variable may be a more important driver of *Ferrovum* abundance than pH. The two *Ferrovum* populations that we detected at Scalp Level Run were inversely correlated with each other and correlated with the concentration of ferrous iron. These correlations lead us to speculate that the concentration of ferrous iron partially controls within-genus niche specificity among *Ferrovum* populations, whereas the pH is a primary driver of abundance among higher-level taxonomic units such as *Ferrovum*, *Gallionella*, and *Acidithiobacillus*. This hypothesis remains to be tested in future work.

MATERIALS AND METHODS

Site location and sample collection. Scalp Level Run (40°14'43.72"N, 78°51'33.18"W) is an acidic coal mine discharge associated with a former bituminous coal mine in Scalp Level Run, Cambria Co., PA. Polluted water discharges from an artesian spring fed by an abandoned mine and flows down a steep hillside and over a coal tailings pile before joining Little Paint Creek (Fig. 1). Five sites were selected along the flow path from the emergence to the base of the coal tailings pile (Fig. 1). Sediment samples for community characterization and water samples for geochemical characterization were collected aseptically at each of the five sites (SL 0, SL 8.5, SL 25, SL 47, and SL 82). Sediment samples were preserved in RNAlater (Qiagen) in the field and stored at -20°C in the lab until analysis.

Geochemistry. Conductivity, oxidation-reduction potential (ORP), pH, dissolved oxygen, and iron concentrations were measured in the field. Dissolved oxygen and ORP were measured using a Hach HQ40d portable meter with an LDO101 dissolved oxygen probe and an MTC101 ORP probe (Hach, Loveland, CO, USA). Temperature, pH, and conductivity were measured using a WTW Multiline pH Conductivity 340 m and associated probes. Ferrous and total iron (method 8008) were measured in the field with a Hach DR 2700 portable spectrophotometer (Hach, Loveland, CO, USA) using the 1,10-phenanthroline method (Hach methods 8146 and 8008, respectively).

Small-subunit rRNA gene library. DNA from environmental samples was obtained using a MoBio Power Biofilm DNA extraction kit (MoBio, Carlsbad, CA, USA). To minimize DNA extraction bias, each sample was extracted twice, with either a 2- or 4-min vortex bead-beating time. The products from the two extractions were pooled. Clone libraries were constructed to obtain nearly full-length 16S rRNA gene

sequences. These sequences were used to clarify the phylogenetic placements of the abundant taxa from the Scalp Level Run community. Small-subunit (16S) rRNA genes were amplified and cloned from the SL emergence sample as described previously (38). Briefly, 16S rRNA genes were amplified using PCR with bacterium-specific primers 27f and 1492r, cloned into chemically competent *Escherichia coli* OneShot Top10 cells. Cells were plated on and grown in agar containing 0.1% kanamycin to select for cells containing the 16S rRNA gene sequences. Inserts were amplified by PCR using T3 and T7 primers and sequenced at the Penn State University Nucleic Acid Facility using plasmid-specific primers. DNA sequences were assembled and manually checked and trimmed in CodonCode Aligner v. 2 (CodonCode Corporation, Dedham, MA, USA) and identified using NCBI Nucleotide BLAST (39). We picked and sequenced 45 clones. From these, we obtained 43 nearly full-length sequences (see below for accession numbers).

Nearly full-length 16S sequences were aligned with ClustalW (40). Phylogenetic trees were constructed using the maximum likelihood method, with the Tamura-Nei nucleotide substitution model (41). Evolutionary analyses were conducted in MEGA7 (42).

High-throughput sequencing was performed on samples SL 8.5, SL 25, and SL 82 using an Illumina MiSeq as described previously (36, 43). Briefly, the V4 region of the 16S rRNA gene was amplified using primers 515f and 806r with attached sequencing barcodes and adaptors and pooled in equimolar quantities for sequencing. We chose to use bacterium-specific primers because *Archaea* composed less than 5% of 4',6-diamidino-2-phenylindole (DAPI)-stained cells (data not shown). Initial quality control was done within the MacQIIME (www.wernerlab.org/software/macqiime) implementation of QIIME 1.7.0 (44). Sequences were split using sample-specific barcodes and trimmed to a minimum *q* score of 20. Sequences were then processed in mothur (45) as described previously (46). Briefly, sequences shorter than 200 bp and longer than 300 bp, sequences with ambiguous bases, and those with homopolymer sequences greater than 8 bp were removed. Sequences were aligned to the Silva nonredundant database (v119) (47). Chimeras were removed using chimera.uchime (48). Chloroplast and mitochondrion sequences were also removed. From each sample, 10,000 sequences were randomly chosen for downstream analysis to allow even comparisons. Operational taxonomic units (OTUs) were picked using a 97% similarity threshold and the nearest-neighbor method. We picked and sequenced 45 clones. From these, we obtained 43 nearly full-length sequences (see below for availability of the demultiplexed and quality-filtered sequences).

Fluorescence *in situ* hybridization and probe design. FISH was performed as described previously (11) on all sediment samples. Briefly, environmental samples were fixed in 4% (wt/vol) paraformaldehyde and stored in a 1:1 ethanol-phosphate-buffered saline (ethanol-PBS) solution at -20°C . Samples were stained with taxon-specific probes (Table 1), counterstained with DAPI (Sigma-Aldrich, Darmstadt, Germany), and viewed using epifluorescence microscopy. A minimum of 1,000 DAPI-stained cells were counted for each probe combination. New FISH probes Xan940 and Ferri836 were designed with sequences from clone libraries from Scalp Level Run and other sites according to the protocol described by Hugenholtz et al. (49) using the PROBE_DESIGN tool in ARB (50). The optimum formamide concentration for Xan940 was determined using Scalp Level Run sample SL 8.5 as a positive control. This sample contains 29% *Xanthomonadales*. *E. coli* was used as a negative control (5-bp mismatches). The Xan940 probe targets a monophyletic clade of *Xanthomonadales* sequences retrieved from acidic or mining-related environments. The optimum formamide concentration for Ferri836 was determined using a culture of *Ferrirothicum radicum*. The Ferri836 probe targets sequences isolated from acidic environments that are closely related to the *Ferrirothicum radicum*. The Ferri836 probe has a 1-bp mismatch to a single nontarget sequence and a 2-bp mismatch to sequences in *Thiobacillus* and *Gallionellales* clades (*Betaproteobacteria*). Unidentified betaproteobacterial sequences were quantified by counting the cells stained by the *Betaproteobacterium*-specific probe Bet42a and subtracting the relative abundance of *Gallionella* and *Ferroplasma*.

Linear regressions were performed in R (51) to test the significance of the relationships between the average relative abundances of taxa.

Niche model. The FISH counts for three AMD taxa (an acidophilic *Gallionella* sp., *Acidithiobacillus ferrooxidans*, and *Ferroplasma myxofaciens*) were retrieved from Jones et al. (13) and Brown et al. (14) and combined with the counts from Scalp Level Run. A local polynomial regression (Loess) curve was fitted to the relationship of pH and relative abundance for each taxon using a span value of 1 in the "loess" command in R (51).

Accession number(s). Unique, nonchimeric 16S rRNA gene sequences were submitted to the NCBI database under accession numbers [KX501140](https://doi.org/10.1128/AEM.00015-17) to [KX501172](https://doi.org/10.1128/AEM.00015-17). Demultiplexed and quality-filtered sequences are available on MG-RAST (accession no. 4672512.3).

SUPPLEMENTAL MATERIAL

Supplemental material for this article may be found at <https://doi.org/10.1128/AEM.00015-17>.

SUPPLEMENTAL FILE 1, PDF file, 0.1 MB.

ACKNOWLEDGMENTS

We thank I. Schaperdoth for laboratory assistance and A. Vikram for technical assistance with sequencing. We thank Melissa Reckner from the Paint Creek Regional Watershed Association for introducing us to the Scalp Level Run site.

REFERENCES

- Johnson DB, Hallberg KB. 2005. Acid mine drainage remediation options: a review. *Sci Total Environ* 338:3–14. <https://doi.org/10.1016/j.scitotenv.2004.09.002>.
- Herlihy AT, Kaufmann PR, Mitch ME, Brown DD. 1990. Regional estimates of acid mine drainage impact on streams in the Mid-Atlantic and South-eastern United States. *Water Air Soil Poll* 50:91–107.
- Tremblay GA, Hogan CM (ed). 2001. Mine environment neutral drainage (MEND) manual 5.4.2d: prevention and control. Canada Centre for Mineral and Energy Technology, Natural Resource Canada, Ottawa, Canada.
- Hudson-Edwards KA, Jamieson HE, Lottermoser BG. 2011. Mine wastes: past, present, future. *Elements* 7:375–380. <https://doi.org/10.2113/gselements.7.6.375>.
- Brady BC, Kania T, Smith WM, Hornberger RJ (ed). 1998. Coal mine drainage prediction and pollution prevention in Pennsylvania. Pennsylvania Department of Environmental Protection, Harrisburg, PA.
- California Mining Waste Study. 1988. Final report. University of California, Berkeley, CA.
- Boyer J, Sarnoski B. 1995. 1995 Progress report—statement of mutual intent strategic plan for the restoration and protection of streams and watersheds polluted by acid mine drainage from abandoned coal mines. Appendix. US EPA, Philadelphia, PA.
- Kirby CS, Brady JAE. 1998. Field determination of Fe²⁺ oxidation rates in acid mine drainage using a continuously-stirred tank reactor. *Appl Geochem* 13:509–520. [https://doi.org/10.1016/S0883-2927\(97\)00077-2](https://doi.org/10.1016/S0883-2927(97)00077-2).
- Sánchez España J, López Pamo E, Santofimia E. 2007. The oxidation of ferrous iron in acidic mine effluents from the Iberian Pyrite Belt (Odiel Basin, Huelva, Spain): field and laboratory rates. *J Geochem Explor* 92:120–132. <https://doi.org/10.1016/j.gexplo.2006.08.010>.
- Senko JM, Wanjugi P, Lucas M, Bruns MA, Burgos WD. 2008. Characterization of Fe(II) oxidizing bacterial activities and communities at two acidic Appalachian coal mine drainage-impacted sites. *ISME J* 2:1134–1145. <https://doi.org/10.1038/ismej.2008.60>.
- Larson LN, Sánchez-España J, Burgos W. 2014. Rates of low-pH Fe(II) oxidation in the Appalachian bituminous coal basin and Iberian pyrite belt. *Appl Geochem* 47:85–98. <https://doi.org/10.1016/j.apgeochem.2014.05.012>.
- Macalady JL, Hamilton TL, Grettenberger CL, Jones DS, Tsao LE, Burgos WD. 2013. Energy, ecology, and the distribution of microbial life. *Philos Trans R Soc Lond B Biol Sci* 68:20120383. <https://doi.org/10.1098/rstb.2012.0383>.
- Jones DS, Kolesar C, Grettenberger CL, Larson LN, Burgos WD, Macalady JL. 2015. Ecological niches of Fe-oxidizing acidophiles in an acidic coal mine drainage. *Appl Environ Microbiol* 81:1242–1250. <https://doi.org/10.1128/AEM.02919-14>.
- Brown JF, Jones DS, Mills DB, Macalady JL, Burgos WD. 2011. Application of a depositional facies model to an acid mine drainage site. *Appl Environ Microbiol* 77:545–554. <https://doi.org/10.1128/AEM.01550-10>.
- Rowe OF, Johnson DB. 2008. Comparison of ferric iron generation by different species of acidophilic bacteria immobilized in packed-bed reactors. *Syst Appl Microbiol* 31:68–77. <https://doi.org/10.1016/j.syapm.2007.09.001>.
- Ziegler S, Waidner B, Itoh T, Schumann P, Spring S, Gescher J. 2013. *Metallibacterium scheffleri* gen. nov., sp. nov., an alkalizing gammaproteobacterium isolated from an acidic biofilm. *Int J Syst Evol Microbiol* 63:1499–1504. <https://doi.org/10.1099/ijs.0.042986-0>.
- Soo RM, Skennerton CT, Sekiguchi Y, Imelfort M, Paech SJ, Dennis PG, Steen JA, Parks DH, Tyson GW, Hugenholtz P. 2014. An expanded genomic representation of the phylum Cyanobacteria. *Genome Biol Evol* 6:1031–1045. <https://doi.org/10.1093/gbe/evu073>.
- Fuchs BM, Wallner G, Beisker W, Schwippl I, Ludwig W, Amann R. 1998. Flow cytometric analysis of the in situ accessibility of *Escherichia coli* 16S rRNA for fluorescently labeled oligonucleotide probes. *Appl Environ Microbiol* 64:4973–4982.
- Hallberg KB, Coupland K, Kimura S, Johnson DB. 2006. Macroscopic streamer growths in acidic, metal-rich mine water in north Wales consist of novel and remarkably simple bacterial communities. *Appl Environ Microbiol* 72:2022–2030. <https://doi.org/10.1128/AEM.72.3.2022-2030.2006>.
- Heinzel E, Janneck E, Glombitza F, Schlömann M, Seifert J. 2009. Population dynamics of iron-oxidizing communities in pilot plants for the treatment of acid mine waters. *Environ Sci Technol* 43:6138–6144. <https://doi.org/10.1021/es900067d>.
- Kimura S, Bryan CG, Hallberg KB, Johnson DB. 2011. Biodiversity and geochemistry of an extremely acidic, low-temperature subterranean environment sustained by chemolithoautotrophy. *Environ Microbiol* 13:2092–2104. <https://doi.org/10.1111/j.1462-2920.2011.02434.x>.
- García-Moyan A, González-Toril E, Aguilera A, Amils R. 2012. Comparative microbial ecology study of the sediments and the water column of the Rio Tinto, an extreme acidic environment. *FEMS Microbiol Ecol* 81:303–314. <https://doi.org/10.1111/j.1574-6941.2012.01346.x>.
- Hur M, Kim Y, Song H, Kim J, Choi Y, Yi I. 2011. Effect of genetically modified poplars on soil microbial communities during the phytoremediation of waste mine tailings. *Appl Environ Microbiol* 77:7611–7619. <https://doi.org/10.1128/AEM.06102-11>.
- Hallberg KB, Johnson DB. 2003. Novel acidophiles isolated from moderately acidic mine drainage waters. *Hydrometallurgy* 71:139–148. [https://doi.org/10.1016/S0304-386X\(03\)00150-6](https://doi.org/10.1016/S0304-386X(03)00150-6).
- Brantner JS, Haake ZJ, Burwick JE, Menge CM, Hotchkiss ST, Senko JM. 2014. Depth-dependent geochemical and microbiological gradients in Fe(III) deposits resulting from coal mine-derived acid mine drainage. *Front Microbiol* 5:215. <https://doi.org/10.3389/fmicb.2014.00215>.
- Yang Y, Wan M, Shi W, Peng H, Qiu G, Zhou J, Liu X. 2007. Bacterial diversity and community structure in acid mine drainage from Dabaoshan Mine, China. *Aquat Microb Ecol* 47:141–151. <https://doi.org/10.3354/ame047141>.
- Sánchez-Andrea I, Stams AJM, Amils R, Sanz JS. 2013. Enrichment and isolation of acidophilic sulfate-reducing bacteria from Tinto River sediments. *Environ Microbiol Rep* 5:672–678. <https://doi.org/10.1111/1758-2229.12066>.
- Tischer K, Kleinstaub S, Schleientz KM, Fetzter I, Spott O, Stange F, Lohse U, Franz J, Neumann F, Gerling S, Schmidt C, Hasselwander E, Harms H, Wendelg A. 2013. Microbial communities along biogeochemical gradients in a hydrocarbon-contaminated aquifer. *Environ Microbiol* 15:2603–2615. <https://doi.org/10.1111/1462-2920.12168>.
- Johnson DB, Hallberg KB, Hedrich S. 2014. Uncovering a microbial enigma: isolation and characterization of the streamer-generating, iron-oxidizing, acidophilic bacterium “*Ferrovum myxofaciens*”. *Appl Environ Microbiol* 80:672–680. <https://doi.org/10.1128/AEM.03230-13>.
- Weiss JV, Rentz JA, Plaia T, Neubauer SC, Merrill-Floyd M, Lilburn T, Bradburne C, Meganigal JP, Emerson D. 2007. Characterization of neutrophilic Fe(II)-oxidizing bacteria isolated from the rhizosphere of wetland plants and description of *Ferritrophicum radicolica* gen. nov. sp. nov., and *Sideroxydans paludicola* sp. nov. *Geomicrobiol. J* 24:559–570. <https://doi.org/10.1080/01490450701670152>.
- He Z, Xiao S, Zhong H, Hu Y, Li Q, Gao F, Li G, Liu J, Qiu G. 2007. Molecular diversity of microbial community in acid mine drainages of Yunfu sulfide mine. *Extremophiles* 11:305–314. <https://doi.org/10.1007/s00792-006-0044-z>.
- He Z, Xiao S, Xie X, Hu Y. 2008. Microbial diversity in acid mineral leaching systems of Dongxiang copper mine and Yinshan lead-zinc mine. *Extremophiles* 12:225–234. <https://doi.org/10.1007/s00792-007-0130-x>.
- Bruneel O, Duran R, Casiot C, Elbaz-Poulichet F, Personne JC. 2006. Diversity of microorganisms in Fe-As-rich acid mine drainage waters of Carnoules, France. *Appl Environ Microbiol* 72:551–556. <https://doi.org/10.1128/AEM.72.1.551-556.2006>.
- Gonzalez-Toril E, Aguilera A, Souza-Egipsy V, Lopez Pamo E, Sanchez Espana J, Amils R. 2011. Geomicrobiology of La Zarza-Perrunal acid mine effluent (Iberian Pyritic Belt, Spain). *Appl Environ Microbiol* 77:2685–2694. <https://doi.org/10.1128/AEM.02459-10>.
- Jew AD, Behrens SF, Rytuba JJ, Kappler A, Spormann AM, Brown GE, Jr. 2014. Microbially enhanced dissolution of HgS in an acid mine drainage system in the California Coast Range. *Geobiology* 12:20–33. <https://doi.org/10.1111/gbi.12066>.
- Sheng Y, Bibby K, Grettenberger CL, Kaley B, Macalady JL, Wang G, Burgos WD. 2016. Geochemical and temporal influences on the enrichment of acidophilic iron-oxidizing bacterial communities. *Appl Environ Microbiol* 82:3611–3621. <https://doi.org/10.1128/AEM.00917-16>.
- Kuang JL, Huang LN, Cgeb LX, Hua ZS, Li SJ, Hu M, Li JT, Shu WS. 2013. Contemporary environmental variation determines microbial diversity patterns in acid mine drainage. *ISME J* 7:1038–1050. <https://doi.org/10.1038/ismej.2012.139>.
- Macalady JL, Dattagupta S, Schaperdorth I, Jones DS, Druschel GK, Eastman D. 2008. Niche differentiation among sulfur-oxidizing bacterial populations in cave waters. *ISME J* 2:590–601. <https://doi.org/10.1038/ismej.2008.25>.

39. Boratyn GM, Camacho C, Cooper PS, Coulouris G, Fong A, Ma N, Madden TL, Matten WT, McGinnis SD, Merezuk Y, Raytselis Y, Sayers EW, Tao T, Ye J, Zaretskaya I. 2013. BLAST: a more efficient report with usability improvements. *Nucleic Acids Res* 41:W29–W33. <https://doi.org/10.1093/nar/gkt282>.
40. Higgins DG, Thompson JD, Gibson TJ. 1994. CLUSTALW: improving the sensitivity of progressive multiple sequence alignment through sequence weighting, position-specific gap penalties and weight matrix choice. *Nucleic Acids Res* 22:4673–4680. <https://doi.org/10.1093/nar/22.22.4673>.
41. Tamura K, Nei M. 1993. Estimation of the number of nucleotide substitutions in the control region of mitochondrial DNA in humans and chimpanzees. *Mol Biol Evol* 10:512–526.
42. Kumar S, Stecher G, Tamura K. 2016. MEGA7: Molecular Evolutionary Genetics Analysis version 7.0 for bigger datasets. *Mol Biol Evol* 33:1870–1874. <https://doi.org/10.1093/molbev/msw054>.
43. Caporaso JG, Lauber CL, Walters WA, Berg-Lyons D, Lozupone CA, Turnbaugh PJ, Fierer N, Knight R. 2011. Global patterns of 16S rRNA diversity at a depth of millions of sequences per sample. *Proc Natl Acad Sci U S A* 108:4516–4522. <https://doi.org/10.1073/pnas.1000080107>.
44. Caporaso JG, Kuczynski J, Stombaugh J, Bittinger K, Bushman FD, Costello EK, Fierer N, Gonzalez Peña A, Goodrich JK, Gordon JI, Huttley GA, Kelley ST, Knights D, Koenig JE, Ley RE, Lozupone CA, McDonald D, Muegge BD, Pirrung M, Reeder J, Sevinsky JR, Turnbaugh PJ, Walters WA, Widmann J, Yatsunenko T, Zaneveld J, Knight R. 2010. QIIME allows analysis of high-throughput community sequence data. *Nat Methods* 7:335–336. <https://doi.org/10.1038/nmeth.f.303>.
45. Schloss PD, Westcott SL, Ryabin T, Hall JR, Hartmann M, Hollister EB, Lesniewski RA, Oakley BB, Parks DH, Robinson CJ, Sahl JW, Stres B, Thallinger GG, Van Horn DJ, Weber CF. 2009. 2009. Introducing mothur: open-source, platform-independent, community-supported software for describing and comparing microbial communities. *Appl Environ Microbiol* 75:7537–7541. <https://doi.org/10.1128/AEM.01541-09>.
46. Kozich JJ, Wescott SL, Baxter NT, Highlander SK, Schloss PD. 2013. Development of a dual-index sequencing strategy and curation pipeline for analyzing amplicon sequence data on the MiSeq Illumina sequencing platform. *Appl Environ Microbiol* 79:5112–5120. <https://doi.org/10.1128/AEM.01043-13>.
47. Quast C, Pruesse E, Yilmaz P, Gerken J, Schweer T, Yarza P, Peplies J, Glöckner FO. 2013. The SILVA ribosomal RNA gene database project: improved data processing and web-based tools. *Nucleic Acids Res* <https://doi.org/10.1093/nar/gks/1210>.
48. Edgar RC. 2010. Search and clustering orders of magnitude faster than BLAST. *Bioinformatics* 26:2460–2461. <https://doi.org/10.1093/bioinformatics/btq461>.
49. Hugenholtz P, Tyson GW, Blackwell LL. 2002. Design and evaluation of 16S rRNA-targeted oligonucleotide probes for fluorescence in situ hybridization. *Methods Mol Biol* 179:29–42.
50. Ludwig W, Strunk O, Westram R, Richter L, Meier H, Yadhukumar Buchner A, Lai T, Steppi S, Jobb G, Förster W, Brettske I, Gerber S, Ginhart A, Gross O, Grumann S, Hermann S, Jost R, König A, Liss T, Lüßmann R, May M, Nonhoff B, Reichel B, Strehlow R, Stamatakis A, Stuckmann N, Vilbig A, Lenke M, Ludwig T, Bode A, Schleifer KH. 2004. ARB: a software environment for sequence data. *Nucleic Acids Res* 32:1363–1371. <https://doi.org/10.1093/nar/gkh293>.
51. R Core Development Team. 2015. R: a language and environment for statistical computing. R Foundation for Statistical Computing, Vienna Austria. <https://www.R-project.org/>.
52. Amann RI, Binder BJ, Olson SW, Chisholm SW, Devereux R, Stahl DA. 1990. Combination of 16S rRNA-targeted oligonucleotide probes with flow cytometry for analyzing mixed microbial populations. *Appl Environ Microbiol* 56:1919–1925.
53. Daims H, Brühl R, Amann R, Schleifer KH, Wagner M. 1999. The domain-specific probe EUB338 is insufficient for the detection of all Bacteria: development and evaluation of a more comprehensive probe set. *Syst Appl Microbiol* 22:434–444. [https://doi.org/10.1016/S0723-2020\(99\)80053-8](https://doi.org/10.1016/S0723-2020(99)80053-8).
54. Gonzalez-Toril E, Llobet-Brossa E, Casamayor EO, Amann R, Amils R. 2003. Microbial ecology of an extreme acidic environment, the Tinto River. *Appl Environ Microbiol* 69:4853–4865. <https://doi.org/10.1128/AEM.69.8.4853-4865.2003>.
55. Manz W, Amann R, Ludwig W, Wagner M, Schlepper KH. 1992. Phylogenetic oligodeoxynucleotide probes for the major subclasses of Proteobacteria: problems and solutions. *Syst Appl Microbiol* 15:593–600. [https://doi.org/10.1016/S0723-2020\(11\)80121-9](https://doi.org/10.1016/S0723-2020(11)80121-9).